# A Human Dynamin-related Protein Controls the Distribution of Mitochondria

**Elena Smirnova, Dixie-Lee Shurland, Sergey N. Ryazantsev, and Alexander M. van der Bliek**

Department of Biological Chemistry, UCLA School of Medicine, Los Angeles, California 90095-1737

***Abstract.*** Mitochondria exist as a dynamic tubular network with projections that move, break, and reseal in response to local environmental changes. We present evidence that a human dynamin-related protein (Drp1) is specifically required to establish this morphology. Drp1 is a GTPase with a domain structure similar to that of other dynamin family members. To identify the function of Drp1, we transiently transfected cells with mutant Drp1. A mutation in the GTPase domain caused profound alterations in mitochondrial morphology. The tubular projections normally present in wild-type cells were retracted into large perinuclear aggregates in cells expressing mutant Drp1. The morphology of other organelles was unaffected by mutant Drp1. There was also no effect of mutant Drp1 on the transport functions of the secretory and endocytic pathways. By EM, the mitochondrial aggregates found in cells that were transfected with mutant Drp1 appear as clusters of tubules rather than a large mass of coalescing membrane. We propose that Drp1 is important for distributing mitochondrial tubules throughout the cell. The function of this new dynamin-related protein in organelle morphology represents a novel role for a member of the dynamin family of proteins.

Key words: GTPase • mitochondrial morphology • dnm1



The dynamins are a family of structurally similar but functionally diverse GTP-binding proteins with sizes ranging from 70 to 100 kD. The best-characterized class of dynamin family members functions in membrane traffic and includes dynamin and yeast vacuolar protein sorting factor (vps1; De Camilli et al., 1995; Rothman et al., 1990; Schmid, 1997; Urrutia et al., 1997). Dynamin assembles into a multimeric spiral at the neck of clathrin-coated pits where it may pinch vesicles off from the plasma membrane (Takei et al., 1995). This view is supported by biochemical, cell culture, and genetic data. The link to endocytosis was made with the discovery that *Drosophila shibire* defects were caused by mutations in the dynamin gene (Chen et al., 1991; van der Bliek and Meyerowitz, 1991). *Shibire* mutants are rapidly paralyzed when the pool of synaptic vesicles is depleted by a temperature-sensitive block in recycling via clathrin mediated endocytosis (Kessel et al., 1989; Narita et al., 1989; Poodry and Edgar, 1979).

Mammalian cells transfected with a dominant dynamin mutant are similarly blocked in endocytosis (Herskovits et al., 1993; van der Bliek et al., 1993). Nerve termini incubated with GTP-γS show tubular invaginations coated with dynamin spirals, apparently frozen in the act of pinching off (Takei et al., 1995). Purified dynamin was also shown to form spirals in vitro, and some of these spirals appear partially constricted (Hinshaw and Schmid, 1995). More recently, it was shown that brain cytosol forms tubules and purified dynamin forms vesicles when incubated with exogenous membrane (Sweitzer and Hinshaw, 1998; Takei et al., 1998). Earlier electron micrographs of *shibire* flies showed electron-dense collars at the necks of budding vesicles (Kosaka and Ikeda, 1983), but their significance was appreciated only after the discovery of dynamin spirals. Constriction of the spiral may provide the force that pinches vesicles off from the plasma membrane.

Much less is known about the other dynamin family members. The MX proteins are interferon-induced proteins that inhibit viral replication in vertebrate animals (Arnheiter and Meier, 1990), but their mechanism of action is unclear. There is a growing number of other dynamin-related proteins that may have novel membrane functions. These include dnm1 (a potential endosomal trafficking factor in yeast; Gammie et al., 1995), phragmoplastin (a plant septation factor; Gu and Verma, 1996), and Mgm1 (a yeast protein affecting mitochondria; Jones and Fangman, 1992).

All dynamin family members have a highly conserved

Address all correspondence to Alexander M. van der Bliek, Department of Biological Chemistry, UCLA School of Medicine, PO Box 951737, Los Angeles, CA 90095-1737. Tel.: (310) 825-9779. Fax: (310) 206-5272. E-mail: avan@mednet.ucla.edu

$NH_2$-terminal GTPase domain followed by a conserved middle domain and a putative helical domain that we call the assembly domain (see Fig. 1). In addition, most family members have divergent segments. For example, dynamin has a pleckstrin homology domain and a proline-rich domain that mediate interactions with other molecules in clathrin-coated pits (Okamoto et al., 1997; Scaife and Margolis, 1997). The inserted segments of the remaining dynamin family members have no detectable similarity to each other or to other proteins. It seems likely that these divergent inserts help determine the specific functions of the different dynamin family members.

Here we describe the molecular and functional characterization of a human dynamin-related protein (Drp1).[1] This new protein has the same overall structure as other dynamin family members, but no known function. By systematically testing the effects of dominant interfering mutations in Drp1 on the morphologies and functions of a range of organelles, we discovered that Drp1 is important for distributing mitochondria throughout the cytoplasm. This distributing activity represents a novel function for a member of the dynamin family of proteins.

## Materials and Methods

### Molecular Cloning and Sequence Analysis

The complete coding sequence was determined from ESTs obtained from Research Genetics, Inc. (Huntsville, AL) and from a full-length cDNA that was isolated by screening a human stromal cell library kindly provided by J. Boulter (UCLA, Los Angeles, CA). Sequence analysis was by primer-hopping with an ABI Sequencer (Perkin-Elmer Corp., Norwalk, CT). Amplification to add epitope tags or to introduce mutations was done with Pfu polymerase (Stratagene, La Jolla, CA). New clones were sequenced to rule out errors introduced by PCR. A multitissue RNA blot from CLONTECH Laboratories, Inc. (Palo Alto, CA) was hybridized with radiolabeled cDNA corresponding to the carboxy terminal half of the protein. The mammalian expression constructs were made with pcDNA3 (Invitrogen Corp., Carlsbad, CA). The ER marker was a transfected vesicular stomatitis virus glycoprotein (VSV-G) cDNA, kindly provided by W.E. Balch (Scripps Research Institute, La Jolla, CA), to which we added an ER retention signal (KKTN) by PCR. This PCR fragment was recloned in pcDNA3. The marker for early endosomes was transfected rab5 to which a myc epitope had been added. A plasmid encoding VSV-G tsO45 with GFP (Presley et al., 1997) was kindly provided by J.F. Presley and J. Lippincott-Schwartz (National Institutes of Health, Bethesda, MD).

### Cell Culture and Transfection Procedures

COS-7 cells were grown in DMEM with 10% FCS. Transfections were done by electroporation and cells were allowed to recover for 48 h. Methods for the VSV-G tsO45 GFP temperature shift experiment were described previously (Presley et al., 1997). The endocytosis experiments were performed by incubating cells at 37°C with serum-free medium and 10 μg/ml Bodipy FL low-density lipoprotein (LDL) or 20 μg/ml Bodipy FL transferrin (Molecular Probes, Inc.). The LDL-treated cells were processed for immunofluorescence after 25 min. The transferrin-treated cells were processed after 60 and 120 min.

### Antibodies and Immunofluorescence Procedures

A 1150-bp fragment encoding the COOH-terminal half of dynamin-related protein was generated by PCR using primers that add an NcoI site to the 5′-end and a SalI site to the 3′-end. This fragment was recloned into the bacterial expression vector pET21d (Novagen Inc., Madison, WI), which adds six histidines to the carboxy terminus. The plasmid was expressed in *Escherichia coli* strain BL21DE3, and the 42-kD recombinant protein, which extends from the glutamic acid residue at position 359 to the carboxy-terminal end of Drp1, was purified by Ni-NTA chromatography. Chicken antisera were generated by Aves Labs (Tigard, OR) and then blot-purified with recombinant Drp1 protein fragment (Harlow and Lane, 1988). For Western blotting the proteins were size-fractionated on a 10% SDS-PAGE gel and transferred to nitrocellulose by standard procedures (Harlow and Lane, 1988). Blotted proteins were detected by chemiluminescence (Nycomed Amersham, Buckinghamshire, England). Protein extracts of human tissues were obtained from CLONTECH Laboratories, Inc. (Palo Alto, CA). Cells grown on coverslips were fixed for immunofluorescence with methanol/acetone or with paraformaldehyde. W.E. Balch (Scripps Research Institute) kindly provided anti-sec13 antibodies. The following primary antibodies were purchased: anti-HA (HA11), anti-dynamin and anti-myc (9E10) from BAbCO Inc. (Richmond, CA), anti-VSV-G and anti-β-COP from Sigma Chemical Co. (St. Louis, MO), anti-COXI from Molecular Probes, Inc. (Eugene, OR), anti-LAMPI from PharMingen (San Diego, CA), and anti-catalase from Calbiochem-Novabiochem Corp. (La Jolla, CA).

### Electron Microscopy

COS-7 cells were transfected with Drp1 encoding plasmids using FuGENE (Boehringer Mannheim GmbH, Mannheim, Germany) and grown on coverslips for 26 hours. The cells were then washed with PBS, fixed with 2% glutaraldehyde (Ted Pella Inc., Redding, CA), washed again with PBS, and incubated for 1 h with 2% osmium tetroxide in 100 mM Na-cacodylate (pH 7.4). This treatment was followed by washing with the cacodylate buffer and an incubation with 1% uranyl acetate. The samples were then dehydrated and embedded in Epon-812 resin (Robinson et al., 1987), and 4–5-nm sections were prepared with an ultramicrotome (MT-6000-XL; RMC, Tucson, AZ) and mounted on 150 mesh EM grids coated with collodion film. The sections were then stained with uranyl acetate and lead citrate (Robinson et al., 1987) and viewed with a JEM 1200-EX electron microscope (JEOL, Tokyo, Japan) using a 50-μm aperture, 80 kV acceleration, and 3,000–5,000-fold magnification.

## Results

### Sequence of the Dynamin-related Protein, Drp1

We set out to determine the function of a new dynamin-related protein that we call Drp1, but has alternatively been called DVLP1, Dymple, DLP1, and DRP1 by others (Imoto et al., 1998; Kamimoto et al., 1998; Shin et al., 1997; Yoon et al., 1998). Fragments of Drp1 sequence that appeared as ESTs in GenBank were used to screen human cDNA libraries. We isolated cDNAs containing the complete coding sequence of human Drp1. We found that these encode a protein of 699 amino acids (80 kD) with an $NH_2$-terminal GTPase domain similar to other members of the dynamin family. Brain Drp1 has a 37–amino acids exon inserted at position 533 by alternative splicing (Fig. 1). Sequence alignments of the dynamin-related protein have been described (Kamimoto et al., 1998; Shin et al., 1997; Yoon et al., 1998). Overall, the sequence of human Drp1 is most closely related to a *Caenorhabditis elegans* dynamin-related protein designated T12E12.4 in *C. elegans* genomic sequence (62% amino acid identity; see Fig. 1). Among published sequences, the similarity of human Drp1 is greatest to yeast Dnm1p (46% identity; Gammie et al., 1995). The degree of similarity is slightly less to yeast Vps1p (43% identity; Rothman et al., 1990) and other dynamin family members that are important for vesicular traffic (e.g., 40% identity with human dynamin I; van der Bliek et al., 1993). The sequence that replaces the dynamin

1. *Abbreviations used in this paper*: Drp1, dynamin-related protein; GFP, green fluorescent protein; LDL, low-density lipoprotein; VSV-G, vesicular stomatitis virus glycoprotein.

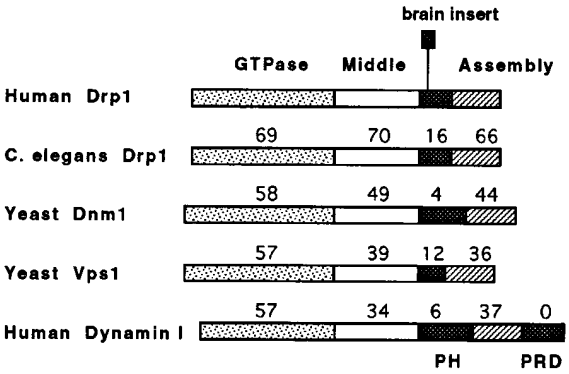


*Figure 1.* Structure of dynamin-related protein and comparison with other dynamin family members. Boundaries of the Drp1 domains were as follows: the GTPase domain was from position 1–300 in the amino acid sequence, the middle domain was from position 301–508, the divergent domain was from position 509–598, and the assembly domain was from position 599–699. Numbers above the individual domains show the percentage identity to the corresponding sequence of the nonneuronal isoform of Drp1.

PH domain is a highly diverged segment of 90 amino acids that may confer specificity to Drp1 function (Fig. 1).

### *Expression Pattern and Subcellular Localization of Drp1*

The Drp1 mRNAs in most human tissues are 2,800 and 4,800 nucleotides (Fig. 2) with the same coding sequence but different polyadenylation sites (not shown). This is different from rat, which has a dominant 4.6-kb mRNA (Yoon et al., 1998). Both of the human Drp1 mRNAs are slightly larger in brain, consistent with insertion of the alternative exon described above (Fig. 2, *inset*). The levels of Drp1 mRNAs are high in brain, moderate in skeletal and heart muscle, and low in other tissues (Fig. 2). Western blot analysis showed that brain Drp1 was slightly larger than nonneuronal Drp1, consistent with the insertion of an alternatively spliced exon (Fig. 3 *A*).

Endogenous Drp1 was difficult to detect by immunofluorescence. COS-7 cells that overexpress transfected Drp1 show primarily cytosolic immunofluorescence (Fig. 3, *B* and *C*). There was no detectable organelle association, even upon treatment with digitonin or streptolysin-O, which was intended to expose small amounts of Drp1 bound to organelles by washing out soluble protein (not shown). Two other studies of Drp1 immunofluorescence have also revealed cytosolic staining (Kamimoto et al., 1998; Shin et al., 1997). In a third study, a fraction of Drp1 was found to colocalize with ER, but most of the protein was cytosolic as well (Yoon et al., 1998).

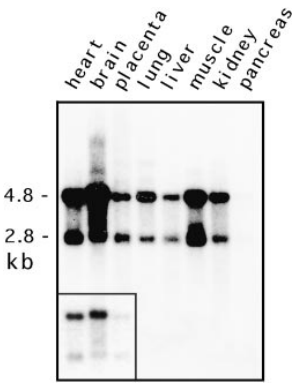


*Figure 2.* Tissue-specific expression of human Drp1. A blot with 2 mg poly A+ RNA from each of the designated human tissues was hybridized with a radiolabeled Drp1 cDNA probe and processed for autoradiography. The mRNA sizes were estimated to be 2.8 and 4.8 kb, corresponding to the usage of different polyadenylation sites. Both mRNAs were ~100 nt longer in brain (*inset* shows a lighter exposure).

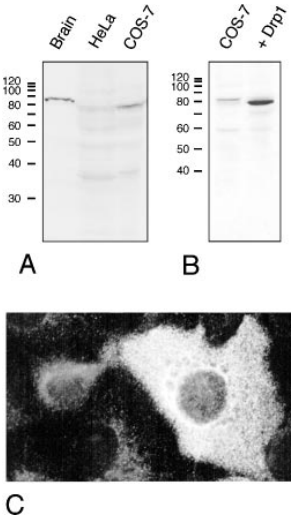


*Figure 3.* (*A*) Immunoblot analysis of Drp1 in protein extracts from bovine brain, HeLa cells, and COS-7 cells, showing a prominent Drp1 band in brain. (*B*) Immunoblot analysis of untransfected COS-7 cells and COS-7 cells transfected with Drp1, showing overexpression of Drp1 in transfected cells. It is unclear whether the faint band in untransfected COS-7 cells represents a slightly larger splice variant of Drp1 or an unrelated protein that cross-reacts with the Drp1 antibody. (*C*) Indirect immunofluorescence of COS-7 cells with anti-Drp1 antibody. The brightly fluorescent cell on the right overexpresses Drp1, which indicates that this cell was a transfectant.

### *Mutant Drp1 has no Effect on Secretory or Endocytic Pathways*

Because of the suggestion that Drp1 might play a role in vesicular traffic (Imoto et al., 1998; Kamimoto et al., 1998; Shin et al., 1997; Yoon et al., 1998), we tested directly whether the transport function of the secretory pathway is impaired by transfecting mutant Drp1 into COS-7 cells. The K38A mutation in Drp1 is analogous to the dynamin K44A mutation that exhibits dominant interfering activity in transiently transfected cells (van der Bliek et al., 1993). We cotransfected K38A mutant Drp1 together with a temperature-sensitive mutant of VSV-G tagged with GFP (Presley et al., 1997). We monitored the progression of GFP fluorescence from ER to Golgi and onto plasma membrane. This experiment showed no difference in the transport of VSV-G through the secretory pathway of cells transfected either with mutant or with wild-type Drp1 (Fig. 4). In agreement with this finding, anti-Drp1 antibody did not affect ER vesicle formation in vitro (W.E. Balch, personal communication). We conclude that the secretory pathway was not affected by mutant Drp1.

We also tested the endocytic pathway in cells that were transfected with mutant Drp1. The transfected cells were incubated with fluorescent LDL in order to assess endocytic function. Accumulation of fluorescence in lysosomes indicated successful transfer of LDL from the plasma membrane to endosomes and onto lysosomes. There was no difference between cells transfected with K38A mutant or with wild-type Drp1, while mutant dynamin clearly blocked LDL uptake (compare the transfected cells that are outlined in Fig. 5 with adjacent untransfected cells).

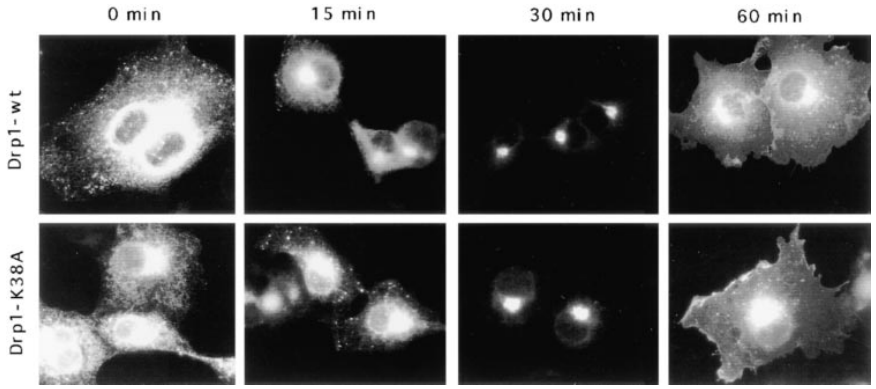


*Figure 4.* Absence of an effect of mutant Drp1 on the secretory pathway. The function of the secretory pathway was monitored by cotransfecting wild-type or mutant Drp1, together with a chimera containing VSV-G tsO45 fused to GFP (Presley et al., 1997). Overexpression of mutant or wild-type Drp1 was verified by double labeling with anti-Drp1 antibody (not shown). The VSV-G chimera was accumulated in the ER by growing transfected cells at 40°C. At 0 min the cells were transferred to the permissive temperature (32°C), allowing the VSV-G chimera to exit the ER. At 15 and 30 min, most of the label was concentrated in the Golgi, and at 60 min most of the label was transferred to the plasma membrane. There was no detectable difference between cells transfected with mutant or wild-type Drp1.

The distribution of fluorescently labeled transferrin, which is taken from the plasma membrane to early endosomes and then recycled back, was also no different in cells transfected with K38A mutant or wild-type Drp1 (not shown), demonstrating that endocytosis was not affected by mutant Drp1.

### *Transfected Drp1 Affects Mitochondria, but not Other Organelles*

To test whether some other aspect of organelle function was affected by mutant Drp1, we investigated the morphology and subcellular distribution of all membrane-bounded organelles in COS-7 cells transfected with K38A mutant Drp1. The ER network was detected by immunostaining of cotransfected VSV-G to which we had attached an ER-retention signal (KKTN at the COOH terminus). Expression of Drp1 containing the K38A mutation had no visible effect on the reticulum (Fig. 6, compare *1* and *2*). The ER bud sites of COPII-coated vesicles that appear clustered near the Golgi, were detected with anti-sec13 antibody (Bannykh et al., 1996). Their distribution was unaltered by Drp1 containing the K38A mutation (compare the transfected cells, which are outlined in of Fig. 6, *3* and *4* with adjacent untransfected cells). The bud sites of COPI-coated vesicles, which were detected with anti-β-COP antibody, were localized to the Golgi. Their distribution was also unchanged by mutant Drp1 (Fig. 6, *5* and *6*). Lysosomes, which were detected with anti-LAMP1 antibody, were also not affected (Fig. 6, *7* and *8*), nor were early endosomes, detected by cotransfecting epitope-tagged rab5 (not shown) and peroxisomes, detected with anti-catalase antibody (not shown).

We then tested whether Drp1 affects mitochondrial morphology by transfecting mutant Drp1 and staining with an antibody specific for mitochondria. In untransfected cells and in cells transfected with wild-type Drp1, the mitochondria are organized in a perinuclear array with tubular extensions that often reach to the cell periphery (compare the transfected cells, which are outlined in Fig. 7, *1* and *2*, with adjacent untransfected cells). When we transfected mutant Drp1, the mitochondrial network invariably collapsed into large perinuclear aggregates (Fig. 7). Occasionally, a few long tubules were retained, but even in those cells mitochondrial collapse was readily apparent (in Fig. 7, *5* and *6′*). The effect on mitochondrial morphology was the same with the nonneuronal isoform of Drp1 containing the K38A mutation (Fig. 7, *5* and *5′*) and with the brain-specific isoform of Drp1 containing the K38A mutation (Fig. 7, *6* and *6′*). In contrast to mutant Drp1, neither mutant nor wild-type forms of dynamin I altered the morphology of the mitochondrial network (Fig. 7, *3* and *4*), which shows that the observed mitochondrial defect is specifically associated with overexpression of mutant Drp1.

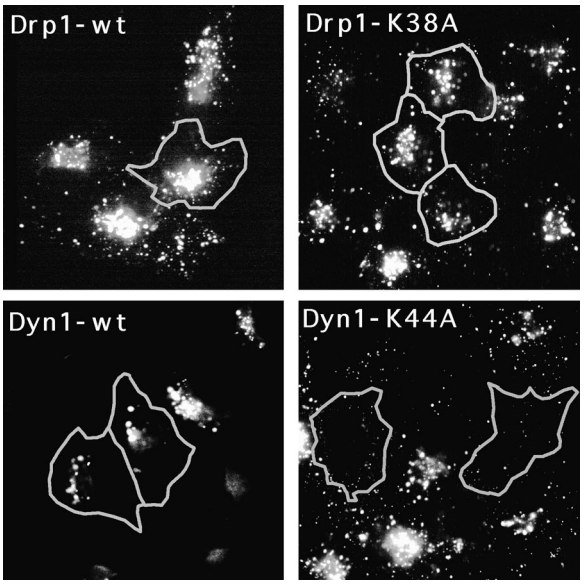


*Figure 5.* Absence of an effect of mutant Drp1 on the endocytic pathway. The function of the endocytic pathway was monitored by following LDL uptake. Cells transfected with the indicated Drp1 or dynamin constructs were incubated at 37°C in serum-free medium with Bodipy-LDL. After 25 min the cells were washed and fixed for staining with anti-Drp1 or anti-dynamin antibody. Cells that overexpress mutant or wild-type Drp1 or dynamin were identified by double labeling with anti-Drp1 or anti-dynamin antibody as indicated by the gray outlines. LDL does not appear in the lysosomes of 70% of cells transfected with mutant dynamin (Dyn1-K44A), demonstrating the validity of this approach. There was no detectable difference in the distribution of lysosomes in cells transfected with wild-type Drp1 (Drp1-wt), the K38A mutant (Drp1-K38A), or in untransfected cells, showing that mutant Drp1 does not affect the endocytic pathway.

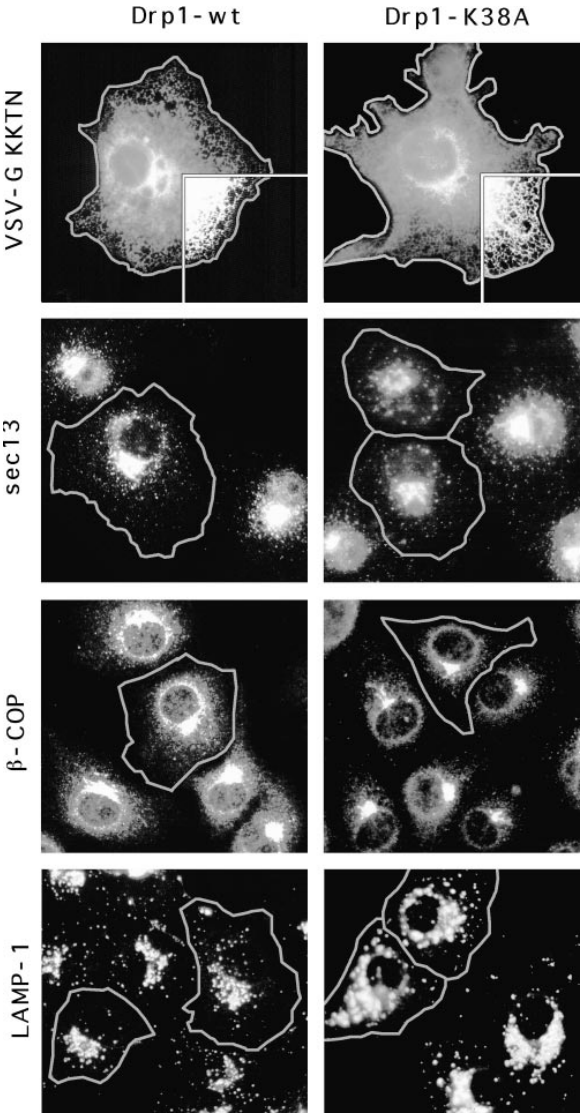


*Figure 6.* Absence of an effect of dominant negative mutant Drp1 on organelles other than mitochondria. Cells that overexpress mutant or wild-type Drp1 were identified by double labeling with anti-Drp1 antibody as indicated by the gray outlines. The ER was detected with an anti-VSV–G antibody by staining cells that were cotransfected with Drp1 and VSV-G carrying an ER retention signal (KKTN at the COOH terminus). The inset shows that the reticulum extends to the cell periphery, both in cells transfected with wild-type (Drp1-wt) and with mutant (Drp1-K38A). COPII-coated vesicles which bud from the ER were detected with anti-sec13 antibody. COPI-coated vesicles, which bud from the Golgi, were detected with anti-β-COP antibody. Lysosomes were detected with anti-LAMP1 antibody. Endosomes detected by cotransfecting epitope-tagged rab5 and peroxisomes detected with anti-catalase antibody were also not affected (not shown).

### *Ultrastructure of Mitochondrial Aggregates Visualized by EM*

To investigate the ultrastructural changes that accompany mitochondrial collapse, we analyzed thin sections of cells transfected with wild-type Drp1 or with Drp1 K38A by EM. An electron micrograph of a typical wild-type cell is shown in Fig. 8 *A*. The mitochondria are dispersed throughout the cytoplasm and appear to be round, ellipsoid, or sausage-shaped depending on the angle of transection through the mitochondrial tubules. We conclude that the mitochondrial tubules have a diameter of ~0.3 μm. In contrast, cells transfected with Drp1 K38A show a cluster of mitochondrial tubules near the nucleus (Fig. 8 *B*). These clusters presumably correspond to the mitochondrial aggregates that were seen by immunofluorescence. In contrast to wild-type cells in which the diameter of mitochondrial tubules was relatively constant, the diameter varied widely in cells transfected with Drp1 K38A (0.1 μm near the center of the cluster, up to 1 μm towards the perimeter of the cluster).

Mitochondria at the perimeter of the clusters were often pleiomorphic with shapes extending from a club or a cup to a ring (Fig. 8 *B*, *2*). In some cases, the ring-shaped mitochondria appeared to make a transition to concentric whorls of cristae (Fig. 8 *B*, *3*). The completed morphological transformation gives these layered structures the appearance of a sliced onion. Similar transformations from club-shaped through ring-shaped and ultimately whorled mitochondria were previously described in the adrenocortex of normal hamsters, in cancer cells, and in cells subjected to noxious conditions (De Robertis and Sabatini, 1958; Ghadially, 1997), but their significance is unknown. Pleiomorphic mitochondria were not always present in cells affected by mutant Drp1, in contrast to the clustering of mitochondrial tubules, which was a constant feature of affected cells. We conclude that the mitochondrial aggregates in cells transfected with mutant Drp1 contain tight clusters of mitochondrial tubules with variable shapes and diameters.

## *Discussion*

Mitochondria have recently attracted attention because of their role in apoptosis (Kluck et al., 1997). There is also a huge body of literature on the role of mitochondria in oxidative phosphorylation, mitochondrial DNA, the transcription/translation machinery, and protein import (Tyler, 1992). However, little or nothing is known about factors contributing to mitochondrial distribution, although this poses fascinating biological problems. It is not widely appreciated that mitochondria exist as an extensive tubular network with projections that move, break, and reseal in response to local environmental changes (Bereiter-Hahn and Voth, 1994; Berger and Yaffe, 1996; Hermann and Shaw, 1998). Our results suggest that Drp1 is specifically required to establish this morphology.

The following observations indicate that mitochondria are the principle target of Drp1 function: (*a*) The collapse of the mitochondrial network is induced by mutant Drp1, but not by mutant dynamin; (*b*) the morphologies of ER, Golgi, endosomes, lysosomes, and peroxisomes are not visibly altered by mutant Drp1; (*c*) the vesicular transport functions of the endocytic and secretory pathways were unaltered by mutant Drp1. The observed effect of Drp1 on mitochondrial morphology is consistent with recent studies in yeast and *C. elegans*. Yeast dnm1 mutants have collapsed mitochondria, suggesting that yeast Dnm1p and human Drp1 are functional equivalents (see the accompanying article by Otsuga et al.). Mitochondria are also col-

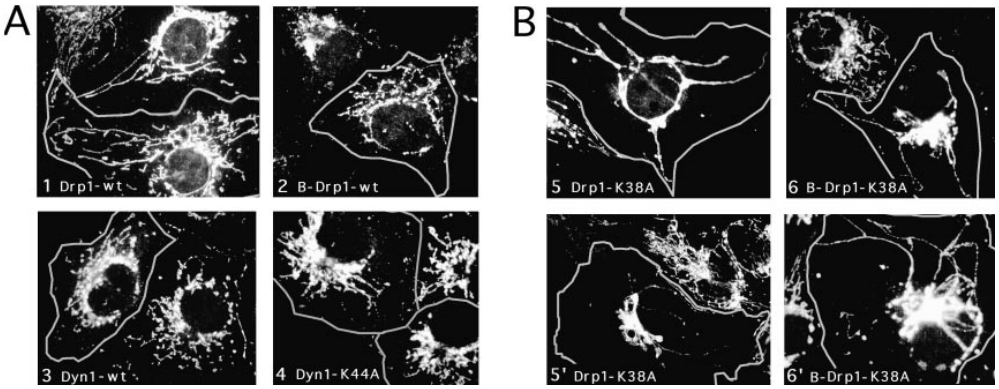


*Figure 7.* Effect of Drp1 on mitochondrial morphology. (*A*) COS-7 cells transfected with wild-type Drp1, wild-type dynamin, or mutant dynamin all show normal mitochondrial morphology. The cells were transfected with Drp1-wt (the nonneuronal isoform; *1*), B-Drp1-wt (the brain-specific isoform of Drp1; *2*), Dyn1-wt (dynamin I wild-type; *3*) or Dyn1-K44A (dynamin I K44A, which blocks endocytosis [van der Bliek et al., 1993]; *4*). The cells were double-labeled with a mitochondrial antibody (anti-COXI) and either anti-Drp1 or anti-dynamin antibody. Outlines of cells that are overexpressing Drp1 or dynamin are superimposed on the mitochondrial staining. Untransfected cells were not outlined. (*B*) COS-7 cells transfected with mutant Drp1 show collapsed mitochondria. Two examples of each condition are shown. The following constructs were tested: Drp1-K38A (the K38A mutant of the non-neuronal isoform; *5* and *5′*), and B-Drp1-K38A (the K38A mutant of the brain specific isoform; *6* and *6′*).



lapsed in *C. elegans* expressing mutant isoforms of *C. elegans* Drp1, although further experiments are required to ensure that this effect is specific (our unpublished results). Functional equivalence is also likely considering the high degree of sequence identity between *C. elegans* and human Drp1 (62% identity, which is remarkably close to the 61% identity between *C. elegans* dyn-1 and human dynamin; Clark et al., 1997). Thus, it seems likely that the mitochondrial function of Drp1 is conserved throughout eukaryotic evolution.

Our localization results are in agreement with previous reports showing that Drp1 is mostly cytosolic (Imoto et al., 1998; Kamimoto et al., 1998; Shin et al., 1997; Yoon et al., 1998). The large fraction of cytosolic protein suggests that Drp1 cycles between the cytosol and a target organelle. A similar cycling occurs with dynamin, which cycles to and from the plasma membrane where it functions in endocytosis (Scaife and Margolis, 1990). In addition, Yoon et al. (1998) observed punctate staining of Drp1 interspersed with punctate ER staining, which led them to suggest that Drp1 is associated with ER. However, it seems unlikely that Drp1 also has an ER-associated function since mutant Drp1 had no effect on ER morphology or on VSV-G transport in our experiments, yet it dramatically changed mitochondrial morphology under the same conditions. Instead, the punctate staining detected by Yoon et al. (1998) may correspond to mitochondria since they are often in close apposition to ER (Bereiter-Hahn and Voth, 1994; Cascarano et al., 1995; Tyler, 1992).

Recently, Imoto et al. (1998) reported transfecting dominant interfering mutant Drp1 and measuring its effect on the secretion of cotransfected luciferase, which they used as a reporter. They found a 50% reduction in secreted luciferase at high concentrations of transfected Drp1 DNA. Since no other cellular functions were tested, it is not possible to assess whether the observed inhibition of secretion was specific. It seems more likely that the inhibitory effect was an indirect consequence of mitochondrial collapse. Cells transfected with high concentrations of mutant Drp1 could have a range of secondary defects because the disruption of mitochondrial morphology might eventually affect oxidative phosphorylation and other vital mitochondrial functions. However, in our comparisons of different cellular functions, the first readily observed defect is the mitochondrial collapse from which we conclude that mitochondria are the principal target of Drp1.

How might Drp1 affect mitochondrial distribution? We envision two alternative explanations. First, Drp1 may help drag mitochondria to the cell periphery. Such a role for Drp1 would complement the well-established role of kinesin in transporting mitochondria along microtubules (Morris and Hollenbeck, 1995). The importance of kinesin was demonstrated by injecting anti-kinesin antibodies, which caused mitochondria to retract from the cell periphery (Rodionov et al., 1993). In addition, some kinesin light chains are specifically associated with mitochondria, where they might serve as adapters to connect mitochondria to a conventional kinesin (Khodjakov et al., 1998). Neurons also possess a specialized kinesin, KIF1B, responsible for axonal transport of mitochondria (Nangaku et al., 1994). KIF1B, like Drp1, is expressed at high levels in the brain, but is different from resident mitochondrial proteins, which are usually expressed at high levels in muscles, but not in the brain (Tiranti et al., 1997). The difference in expression between resident mitochondrial proteins and KIF1B or Drp1 indicates that mitochondrial distribution is more taxing in neurons than in other cell types, regardless of their energy requirements. It is not clear how Drp1 might contribute to mitochondrial motility, if that proves to be its primary function.

Alternatively, Drp1 might affect mitochondrial distribution by helping to pinch off mitochondrial fragments, analogous to the role of dynamin in pinching off clathrin-coated vesicles. To understand how a defect in pinching off might lead to mitochondrial tubule clustering, we propose that normal subcellular distributions require shorter fragments or the separation of branched structures. Two lines of reasoning make a role in pinching seem more likely than a role in transport. First, the structural similarity between dynamin and Drp1 suggests that Drp1 might

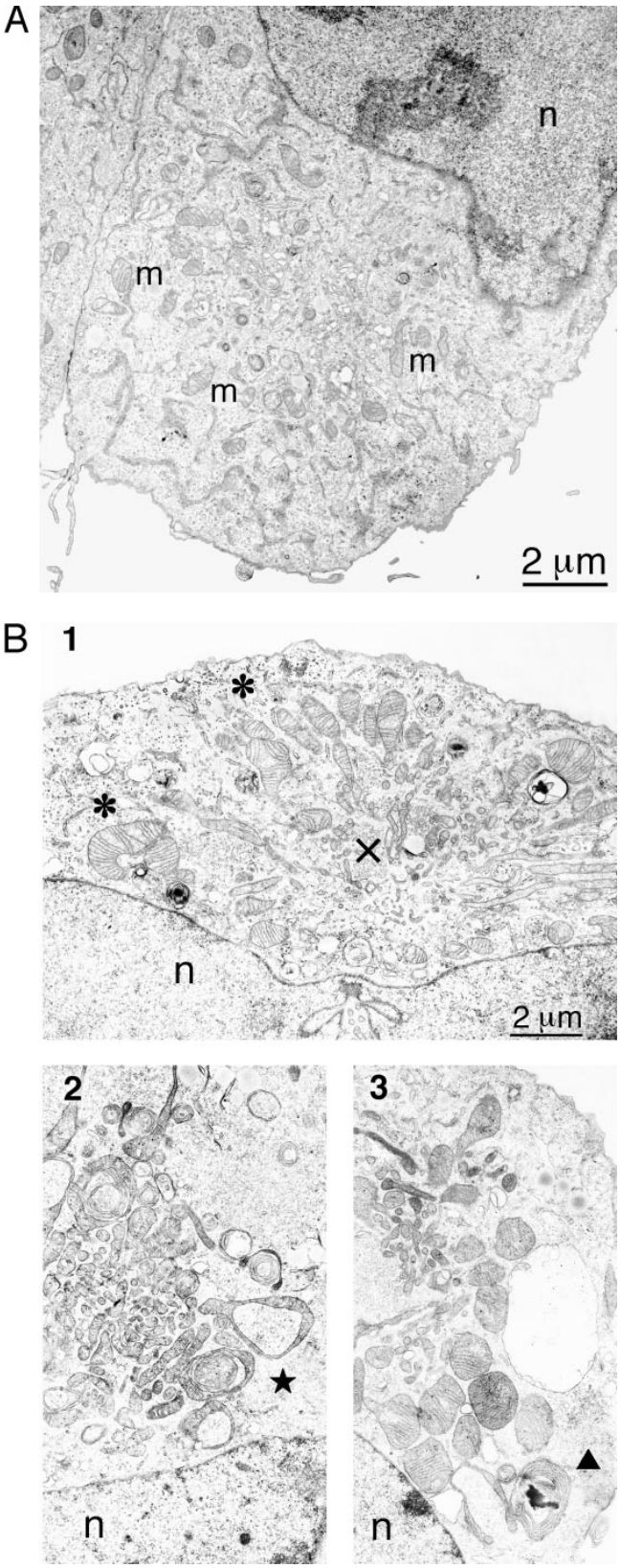


*Figure 8.* EM analysis of COS-7 cells transfected with mutant or wild type Drp1. (*A*) Thin section of a wild-type cell. This cell is a typical example of the cells observed in transfection experiments with wild-type Drp1 in which untransfected cells were indistinguishable from transfected cells. Mitochondria (*m*) are scattered throughout the cytoplasm. The nucleus is visible in the upper part of the panel (*n*). (*B*) Thin sections of cells transfected with K38A mutant Drp1. Each of the three panels shows a cluster of mitochondria near the nucleus (*n*). *1* illustrates the larger diameter of the peripheral mitochondria (∗) and the smaller diameter of the central mitochondria (x). *2* shows ring-like mitochondria (★), which are common in cells transfected with mutant Drp1. *3* shows an onion-like membranous structure (▲) adjacent to a mitochondrial cluster in a cell transfected with mutant Drp1.

form a multimeric complex similar to the dynamin spiral. Second, the cytosolic localization of Drp1 is consistent with a transient role such as the scission of mitochondrial tubules. The lengthened mitochondria resulting from mutant Drp1 might then be too taxing for further distribution throughout the cell. Nothing is known about mitochondrial scission, but it must occur frequently.

The widening of mitochondrial tubules towards the periphery of the clusters in cells transfected with mutant Drp1 may simply help to accommodate the displacement of excess internal matrix from within the cluster of mitochondrial tubules. Mitochondrial clustering may have also induced the odd morphological transformations observed in some of the transfected cells. Club-, cup-, ring-, and onion-shaped mitochondria occur occasionally in normal cell types or under certain adverse conditions (De Robertis and Sabatini, 1958; Ghadially, 1997), which suggests that these abnormalities may be a secondary response to other changes in mitochondrial function. Interestingly, mutations in the *Drosophila fuzzy onions* gene that affects mitochondrial fusion also induce odd cup or ring shapes, supporting the view that these transformations are not directly linked to a single protein function (Hales and Fuller, 1997).

Although it is not yet known how Drp1 might interact with mitochondria, genetic screens conducted with yeast revealed a series of other proteins that affect mitochondrial morphology (Berger and Yaffe, 1996; Hermann et al., 1997; Shepard and Yaffe, 1997). Some of these might interact with Drp1. The order of binding interactions may resemble the recruitment steps needed to form a dynamin spiral at the neck of a budding clathrin coated vesicle (Schmid, 1997). The nature of these interactions will become clear in future studies.

In conclusion, we propose that Drp1 establishes mitochondrial morphology through a role in the distribution of mitochondrial tubules throughout the cytoplasm. Tubule formation and scission contribute to the dynamic nature of mitochondria (Bereiter-Hahn and Voth, 1994; Hermann and Shaw, 1998). Mitochondria can change shape during cell division and during differentiation, for example forming elaborate networks in muscle cells (Tyler, 1992). Mitochondria also rapidly respond to local changes in the intracellular environment, sending out projections that break and reseal elsewhere within seconds (Bereiter-Hahn and Voth, 1994). Our results suggest that Drp1 is a key factor controlling these morphological changes.

We thank the other lab members, G.S. Payne, I.V. Davydov, and P.J. Johnson for valuable suggestions and comments on the manuscript. We thank J. Shaw (University of Utah, Salt Lake City, UT) for sharing unpublished information and for many stimulating discussions. We thank J. Chen and M. Kang for assistance with cDNA cloning and sequence analy-

sis. We thank W.E. Balch (Scripps Research Institute, La Jolla, CA) for testing our anti-Drp1 antibodies in an ER-budding assay, for anti-sec13 antibodies, and for VSV-G plasmid. We thank J.F. Presley and J. Lippincott-Schwartz (National Institutes of Health, Bethesda, MD) for the VSV-G/GFP plasmid and advice on performing the VSV-G transport assay.

This work was supported by grants from the National Institutes of Health (GM 51866), the American Heart Association, and the Cancer Research Coordinating Committee to A.M. van der Bliek. E. Smirnova received fellowships from the Myasthenia Gravis Foundation and the American Heart Association of Greater Los Angeles.

Received for publication 29 June 1998 and in revised form 4 September 1998.

### *References*

Arnheiter, H., and E. Meier. 1990. MX proteins: antiviral proteins by chance or by necessity? *New Biol*. 2:851–857.

Bannykh, S.I., T. Rowe, and W.E. Balch. 1996. The organization of endoplasmic reticulum export complexes. *J. Cell Biol*. 135:19–35.

Bereiter-Hahn, J., and M. Voth. 1994. Dynamics of mitochondria in living cells: shape changes, dislocations, fusion, and fission of mitochondria. *Microsc. Res. Techn*. 27:198–219.

Berger, K.H., and M.P. Yaffe. 1996. Mitochondrial distribution and inheritance. *Experientia*. 52:1111–1116.

Cascarano, J., P.A. Chambers, E. Schwartz, P. Poorkaj, and R.E. Gondo. 1995. Organellar clusters formed by mitochondrial-rough endoplasmic reticulum associations: an ordered arrangement of mitochondria in hepatocytes. *Hepatology*. 22:837–846.

Chen, M.S., R.A. Obar, C.C. Schroeder, T.W. Austin, C.A. Poodry, S.C. Wadsworth, and R.B. Vallee. 1991. Multiple forms of dynamin are encoded by *shibire*, a *Drosophila* gene involved in endocytosis. *Nature*. 351:583–586.

Clark, S.G., D.L. Shurland, E.M. Meyerowitz, C.I. Bargmann, and A.M. van der Bliek. 1997. A dynamin GTPase mutation causes a rapid and reversible temperature-inducible locomotion defect in *C. elegans*. *Proc. Natl. Acad. Sci. USA*. 94:10438–10443.

De Camilli, P., K. Takei, and P.S. McPherson. 1995. The function of dynamin in endocytosis. *Curr. Opin. Neurobiol*. 5:559–565.

De Robertis, E., and D. Sabatini. 1958. Mitochondrial changes in the adrenocortex of normal hamsters. *J. Biophys. Biochem. Cytol*. 4:667–673.

Gammie, A.E., L.J. Kurihara, R.B. Vallee, and M.D. Rose. 1995. DNM1, a dynamin-related gene, participates in endosomal trafficking in yeast. *J. Cell Biol*. 130:553–566.

Ghadially, F.N. 1997. Ultrastructural Pathology of the Cell and Matrix. Vol. 1. Butterworth-Heinemann, Boston. 617 pp.

Gu, X., and D.P.S. Verma. 1996. Phragmoplastin, a dynamin-like protein associated with cell plate formation in plants. *EMBO (Eur. Mol. Biol. Organ.) J*. 15:695–704.

Hales, K.G., and M.T. Fuller. 1997. Developmentally regulated mitochondrial fusion mediated by a conserved, novel, predicted GTPase. *Cell*. 90:121–129.

Harlow, E., and E. Lane. 1988. Antibodies: A Laboratory Manual. Cold Spring Harbor Laboratory, Cold Spring Harbor, NY. 726 pp.

Hermann, G.J., E.J. King, and J.M. Shaw. 1997. The yeast gene, MDM20, is necessary for mitochondrial inheritance and organization of the actin cytoskeleton. *J. Cell Biol*. 137:141–153.

Hermann, G.J., and J.M. Shaw. 1998. Mitochondrial dynamics in yeast. *Annu. Rev. Cell Dev. Biol*. In press.

Herskovits, J.S., C.C. Burgess, R.A. Obar, and R.B. Vallee. 1993. Effects of mutant rat dynamin on endocytosis. *J. Cell Biol*. 122:565–578.

Hinshaw, J.E., and S.L. Schmid. 1995. Dynamin self-assembles into rings suggesting a mechanism for coated vesicle budding. *Nature*. 374:190–192.

Imoto, M., I. Tachibana, and R. Urrutia. 1998. Identification and functional characterization of a novel human protein highly related to the yeast dynamin-like GTPase Vps1p. *J. Cell Sci*. 111:1341–1349.

Jones, B.A., and W.L. Fangman. 1992. Mitochondrial DNA maintenance in yeast requires a protein containing a region related to the GTP-binding domain of dynamin. *Genes Dev*. 6:380–389.

Kamimoto, T., Y. Nagai, H. Onogi, Y. Muro, T. Wakabayashi, and M. Hagiwara. 1998. Dymple, a novel dynamin-like high molecular weight GTPase lacking a proline-rich carboxyl-terminal domain in mammalian cells. *J. Biol. Chem*. 273:1044–1051.

Kessel, I., B.D. Holst, and T.F. Roth. 1989. Membranous intermediates in endocytosis are labile, as shown in a temperature-sensitive mutant. *Proc. Natl. Acad. Sci. USA*. 86:4968–4972.

Khodjakov, A., E.M. Lizunova, A.A. Minin, M.P. Koonce, and F.K. Gyoeva. 1998. A specific light chain of kinesin associates with mitochondria in cultured cells. *Mol. Biol. Cell*. 9:333–343.

Kluck, R.M., E. Bossy-Wetzel, D.R. Green, and D.D. Newmeyer. 1997. The release of cytochrome c from mitochondria: a primary site for Bcl-2 regulation of apoptosis. *Science*. 275:1132–1136.

Kosaka, T., and K. Ikeda. 1983. Possible temperature-dependent blockage of synaptic vesicle recycling induced by a single gene mutation in *Drosophila*. *J. Neurobiol*. 14:207–225.

Morris, R.L., and P.J. Hollenbeck. 1995. Axonal transport of mitochondria along microtubules and F-actin in living vertebrate neurons. *J. Cell Biol*. 131: 1315–1326.

Nangaku, M., R. Sato-Yoshitake, Y. Okada, Y. Noda, R. Takemura, H. Yamazaki, and N. Hirokawa. 1994. KIF1B, a novel microtubule plus end-directed monomeric motor protein for transport of mitochondria. *Cell*. 79: 1209–1220.

Narita, K., T. Tsuruhara, J.H. Koenig, and K. Ikeda. 1989. Membrane pinch-off and reinsertion observed in living cells of *Drosophila*. *J. Cell. Physiol*. 141: 383–391.

Okamoto, P.M., J.S. Herskovits, and R.B. Vallee. 1997. Role of the basic, proline-rich region of dynamin in Src homology 3 domain binding and endocytosis. *J. Biol. Chem*. 272:11629–11635.

Poodry, C.A., and L. Edgar. 1979. Reversible alterations in the neuromuscular junctions of *Drosophila melanogaster* bearing a temperature-sensitive mutation, shibire. *J. Cell Biol*. 81:520–527.

Presley, J.F., N.B. Cole, T.A. Schroer, K. Hirschberg, K.J. Zaal, and J. Lippincott-Schwartz. 1997. ER-to-Golgi transport visualized in living cells. *Nature*. 389:81–85.

Robinson, D.G., U. Ehlers, R. Herken, B. Herrmann, F. Mayer, and F.W. Schurmann. 1987. Methods of Preparation for Electron Microscopy. Springer-Verlag, Berlin, Germany. 190 pp.

Rodionov, V.I., F.K. Gyoeva, E. Tanaka, A.D. Bershadsky, J.M. Vasiliev, and V.I. Gelfand. 1993. Microtubule-dependent control of cell shape and pseudopodial activity is inhibited by the antibody to kinesin motor domain. *J. Cell Biol*. 123:1811–1820.

Rothman, J.H., C.K. Raymond, T. Gilbert, P. O'Hara, and T. Stevens. 1990. A putative GTP binding protein homologous to interferon-inducible Mx proteins performs an essential function in yeast protein sorting. *Cell*. 61:1063–1074.

Scaife, R., and R.L. Margolis. 1990. Biochemical and immunochemical analysis of rat brain dynamin interaction with microtubules and organelles in vivo and in vitro. *J. Cell Biol*. 111:3023–3033.

Scaife, R.M., and R.L. Margolis. 1997. The role of the PH domain and SH3 binding domains in dynamin function. *Cell. Signalling*. 9:395–401.

Schmid, S.L. 1997. Clathrin-coated vesicle formation and protein sorting: an integrated process. *Annu. Rev. Biochem*. 66:511–548.

Shepard, K.A., and M.P. Yaffe. 1997. Genetic and molecular analysis of Mdm14p and Mdm17p, proteins involved in organelle inheritance. *Mol. Biol. Cell*. 8:444*a*.

Shin, H.W., C. Shinotsuka, S. Torii, K. Murakami, and K. Nakayama. 1997. Identification and subcellular localization of a novel mammalian dynamin-related protein homologous to yeast Vps1p and Dnm1p. *J. Biochem*. 122: 525–530.

Sweitzer, S.M., and J.E. Hinshaw. 1998. Dynamin undergoes a GTP-dependent conformational change causing vesiculation. *Cell*. 93:1021–1029.

Takei, K., V. Haucke, V. Slepnev, K. Farsad, M. Salazar, H. Chen, and P. De Camilli. 1998. Generation of coated intermediates of clathrin-mediated endocytosis on protein-free liposomes. *Cell*. 94:131–141.

Takei, K., P.S. McPherson, S.L. Schmid, and P. DeCamilli. 1995. Tubular invaginations coated by dynamin rings are induced by GTP-γS in nerve terminals. *Nature*. 374:186–190.

Tiranti, V., A. Savoia, F. Forti, M.F. D'Apolito, M. Centra, M. Rocchi, and M. Zeviani. 1997. Identification of the gene encoding the human mitochondrial RNA polymerase (h-mtRPOL) by cyberscreening of the Expressed Sequence Tags database. *Hum. Mol. Genet*. 6:615–625.

Tyler, D.D. 1992. The Mitochondrion in Health And Disease. VCH Publishers, Inc., New York. 557 pp.

Urrutia, R., J.R. Henley, T. Cook, and M.A. McNiven. 1997. The dynamins: redundant or distinct functions for an expanding family of related GTPases? *Proc. Natl. Acad. Sci. USA*. 94:377–384.

van der Bliek, A.M., and E.M. Meyerowitz. 1991. Dynamin-like protein encoded by the *Drosophila shibire* gene associated with vesicular traffic. *Nature*. 351:411–414.

van der Bliek, A.M., T.E. Redelmeier, H. Damke, E.J. Tisdale, E.M. Meyerowitz, and S.L. Schmid. 1993. Mutations in human dynamin block an intermediate stage in coated vesicle formation. *J. Cell Biol*. 122:553–563.

Yoon, Y., K.R. Pitts, S. Dahan, and M.A. McNiven. 1998. A novel dynamin-like protein associates with cytoplasmic vesicles and tubules of the endoplasmic reticulum in mammalian cells. *J. Cell Biol*. 140:779–793.